Chemical Science

EDGE ARTICLE

View Article Online
View Journal | View Issue

Cite this: *Chem. Sci.*, 2015, **6**, 335

In vivo visible light-triggered drug release from an implanted depot†

Carl-Johan Carling,[ab] Mathieu L. Viger,[ab] Viet Anh Nguyen Huu,[bc] Arnold V. Garcia[ab] and Adah Almutairi*[abcd]

Controlling chemistry in space and time has offered scientists and engineers powerful tools for research and technology. For example, on-demand photo-triggered activation of neurotransmitters has revolutionized neuroscience. Non-invasive control of the availability of bioactive molecules in living organisms will undoubtedly lead to major advances; however, this requires the development of photosystems that efficiently respond to regions of the electromagnetic spectrum that innocuously penetrate tissue. To this end, we have developed a polymer that photochemically degrades upon absorption of one photon of visible light and demonstrated its potential for medical applications. Particles formulated from this polymer release molecular cargo *in vitro* and *in vivo* upon irradiation with blue visible light through a photoexpansile swelling mechanism.

Received 29th August 2014
Accepted 4th October 2014

DOI: 10.1039/c4sc02651a

www.rsc.org/chemicalscience

Introduction

Controlling chemistry in space and time with light has proven enormously useful in biological research. For example, optogenetics is considered the breakthrough of the decade and has revolutionized neuroscience.[1] However, current means of controlling cellular processes using light require tedious synthetic or genetic development of tools specific to each target. On the other hand, light-responsive nanocarriers[2] can be used to control the activity of any encapsulated bioactive molecule, including proteins and nucleic acids, without the need for chemical modification. Such versatile tools have enormous potential to advance fundamental understanding of physiological, developmental, and disease processes. Externally triggered release of drugs from nanomaterials may also have exciting applications in the treatment of disease, as it could allow precise coordination with biological rhythms or disease activity. Since particles can be injected within the tissue of interest and remain localized in a depot-like manner, the pharmacokinetic profile of the encapsulated drug can be altered. Such an approach would minimize injections and harmful side effects while maximizing therapeutic outcome.

Light-responsive technologies useful *in vivo* must be highly efficient and capable of responding to electromagnetic radiation that can innocuously penetrate into tissue. To date most photochemical systems do not meet such physiological requirements, as the majority rely on UV light activation,[2,3] which is both damaging to cells and does not appreciably penetrate tissues. Systems making use of near-infrared (NIR) laser light by multi-photon approaches, which include two-photon excitation[4] and upconverted UV light,[5] have been developed to sidestep these limitations. Unfortunately, achieving sufficient photocleavage of polymer to induce release from nanoparticles by these approaches currently requires extended irradiation at high laser powers, which could lead to heat-induced damage of biological tissues.[6]

The development of one-photon visible light-responsive carriers[4c,h,i,7] represents an attractive alternative to both one-photon UV- and two-photon NIR-responsive carriers for *in vivo* applications because it is several orders of magnitude more efficient than two-photon excitation,[8] requiring much shorter irradiation times at lower powers, and is less harmful to cells than UV light.

Inspired by recent developments in the photo-uncaging field, we synthesized a polymer that degrades upon one-photon absorption of blue visible light (polymer **1**, Fig. 1, Scheme S1†) by incorporating a recently developed red-shifted photocage developed by Donato *et al.*[8] and used it to formulate particles encapsulating various payloads. Advantages of this photocage over existing systems[3] such as coumarin, nitroveratryls, ruthenium complexes and perylene are the intense visible light absorption up to 500 nm and photo-reactivity in hydrophobic

[a]*Skaggs School of Pharmacy and Pharmaceutical Sciences, University of California, San Diego, 9500 Gilman Dr., La Jolla, California 92093, USA. E-mail: aalmutairi@ucsd.edu; Tel: +1-858-246-0871*

[b]*KACST-UCSD Center for Excellence in Nanomedicine, University of California, San Diego, 9500 Gilman Dr., La Jolla, California 92093, USA*

[c]*Department of NanoEngineering, University of California, San Diego, 9500 Gilman Dr., La Jolla, California 92093, USA*

[d]*Department of Materials Science and Engineering, University of California, San Diego, 9500 Gilman Dr., La Jolla, California 92093, USA*

† Electronic supplementary information (ESI) available: Experimental and synthetic details and additional graphs, chromatograms, photographs and micrographs. See DOI: 10.1039/c4sc02651a

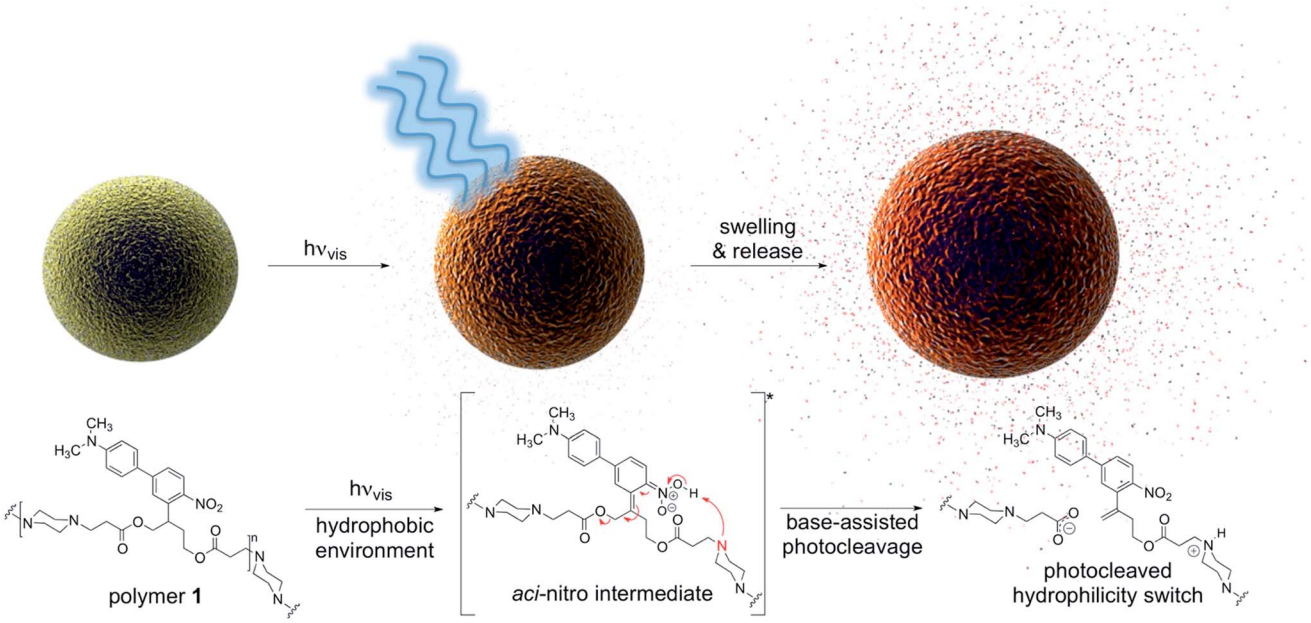

Fig. 1 Visible light irradiation of particles composed of polymer **1** in aqueous media induces swelling and release of molecular cargo. Tertiary amines within the polymer backbone assist deprotonation of the *aci*-nitro intermediate in the hydrophobic particle microenvironment, leading to β-elimination and photocleavage in favour of photorearrangement.

environments, a crucial requirement as most polymer-based delivery vehicles have a hydrophobic interior.

The results presented in this study highlight the practical utility of one-photon visible light photochemistry for applications in dense, non-transparent mammalian tissues. In an *in vivo* mouse model we demonstrate light-triggered drug release from a subcutaneously implanted polymer **1** particle depot with blue visible light.

Results and discussion

Design, light response and degradation mechanism

In this work, the propyloxy chain of the previously reported ANBP[8] (2-(4′-(*N*,*N*-dimethylamino)-4-nitro-[1,1′-biphenyl]-3-yl) propyl carbonyl) photocage was elongated to yield the butanediol derivative 2-(4′-*N*-dimethylamino-4-nitro-[1,1′-biphenyl]-3-yl)butane-1,4-diyl dicarbonyl (ANBB, Fig. 1 and 2, Scheme S1†). This modification facilitates polymerization and enhances the kinetics of photodegradation by placing the photolabile bond directly in the polymer backbone (Fig. 1).[4i,9] Like ANBP, ANBB is photochemically active in hydrophobic environments. As previously reported, the photochemistry of this class of photoresponsive molecules is strongly dependent on solvent and basicity.[10] In water, the photo-induced *aci*-nitro intermediate (Fig. 1) is deprotonated, causing the compound to undergo photocleavage by a β-elimination pathway to yield a nitro-alkene derivative.[8] However, in hydrophobic non-basic environments, these molecules photorearrange to a hydroxy-nitroso isomer[10] (Fig. 2). To increase the release efficiency from corresponding particles and potentially enhance metabolism/excretion of the photodegraded carrier material, we reasoned that the introduction of basic tertiary amines in the polymer **1** backbone would assist deprotonation of the photo-induced *aci*-nitro intermediate in the hydrophobic particle microenvironment in favour of photorearrangement (Fig. 1, 2c and d). To inform the design of our polymer, we examined the photoreactions of model compounds **2** (no tertiary amines) and **3** (tertiary amines) in hydrophobic solvent to mimic the particle microenvironment (Fig. 2, Scheme S1†). As revealed by HPLC-MS, the non-basic compound **2** yielded only the photostable photorearranged nitroso-hydroxy isomer **2a** upon irradiation with visible light (λ_{ex} = 400–500 nm) in CH_2Cl_2 (Fig. 2a and b), whereas the basic compound **3** underwent a much more complex photoreaction (Fig. 2c and d). Analysis of the photoreaction of compound **3** revealed that the major reaction product was indeed the photocleaved nitro-alkene derivative **3a**, which was isolated and identified by ^{1}H NMR spectroscopy (Fig. S1†) and high-resolution mass spectroscopy. However, compound **3** was also observed to directly generate the photorearranged hydroxy-nitroso minor product **3b**, alongside a photocleaved minor product **3c** upon irradiation (Fig. 2c and d). Furthermore, as has been previously observed with similar compounds,[10] the photocleaved nitro-alkene product **3a** is not photostable and undergoes multiple subsequent photochemical transformations upon prolonged irradiation (Fig. 2c and d). Despite considerable efforts, secondary photoproducts (**3c**, **3d**, **3e** and minor products) could not be identified. The observed photochemical behavior of compound **3** confirms that the introduction of tertiary amines indeed promotes photocleavage in hydrophobic environments, such as the interior of a polymeric particle.

The photoresponsive polymer **1** (M_w = 31.7 kDa, PDI = 2.7) was synthesized in five steps at 17% overall yield starting from a previously reported compound[8] (see ESI and Scheme S1† for

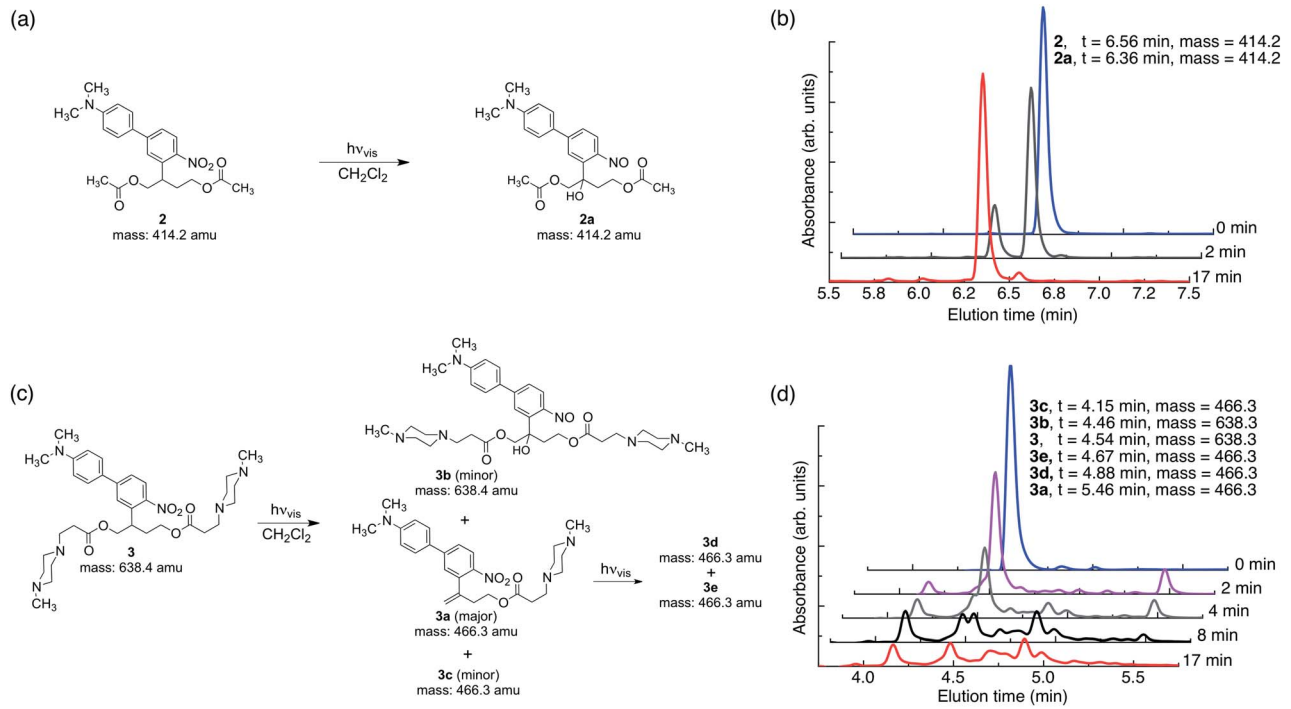

Fig. 2 Tertiary amines modulate the photochemistry of ANBB in hydrophobic environments. (a and b) Compound **2** cleanly reacts upon irradiation with visible light (λ_{ex} = 400–500 nm, 0.18 W, 0.21 W cm^{-2}) in CH_2Cl_2 (6×10^{-5} M) to yield photorearranged hydroxy-nitroso product **2a**. (c and d) Compound **3** has more complex photochemistry and yields photocleaved **3a** (major product), photorearranged **3b** (minor product) and photocleaved **3c** (minor product) upon irradiation with visible light in CH_2Cl_2. **3a** is not photostable and reacts further upon prolonged irradiation to yield major photoproducts **3d** and **3e**. The exact mass calculated (**2**, **2a**, **3**, **3a** and **3c**) and measured (**2**, **2a**, **3a**, **3b**, **3c**, **3d** and **3e** (mass of protons subtracted)) is indicated.

synthetic details). Upon irradiation of polymer **1** in CH_2Cl_2 with visible light (λ_{ex} = 400–500 nm), the long-wavelength absorption peak at λ_{max} = 398 nm decreases as a new absorption peak at λ_{max} = 458 nm increases, resulting in a visually recognizable color change from yellow to orange (Fig. 3a inset). The substantial increase in the GPC retention time of polymer **1** after irradiation in CH_2Cl_2 indicates amine-assisted photocleavage upon irradiation and the formation of smaller segments (Fig. 3b). The greater solubility of the photoproducts of polymer **1** in methanol and in water containing 1% w/v Pluronic® F127 further indicates photodegradation into smaller, more polar segments (Fig. S2†).

HPLC-MS analysis of the methanol-soluble photodegraded material revealed a complex mixture of photoproducts, including peaks with masses corresponding to the smallest photocleaved products anticipated (Fig. S3†). We also studied

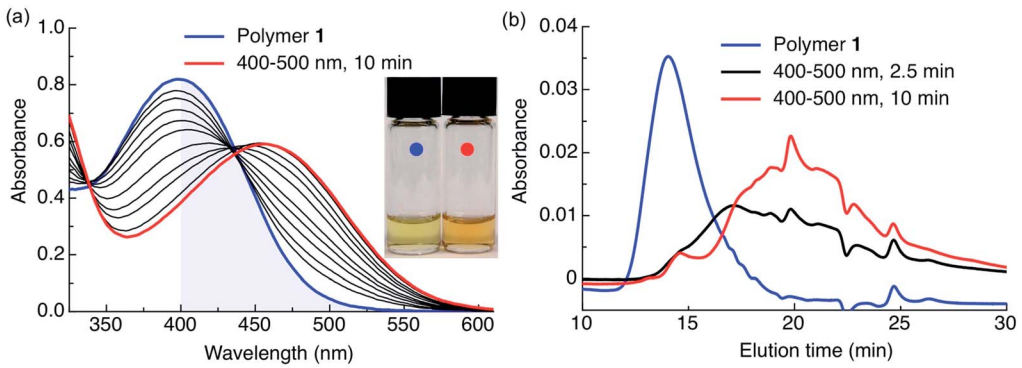

Fig. 3 Polymer **1** photodegrades upon irradiation with visible light in hydrophobic environments. (a) Spectral changes in the UV-Vis spectrum of polymer **1** irradiated in CH_2Cl_2 (0.04 mg mL^{-1}, 0.5 mL) with visible light (λ_{ex} = 400–500 nm, 0.18 W, 0.21 W cm^{-2}). The blue shaded area highlights visible light absorption. Inset: color change following complete photoconversion. (b) GPC chromatogram of polymer **1** before (blue trace, M_w = 31.7 kDa, PDI = 2.7, PMMA standard) and after irradiation in CH_2Cl_2 (0.04 mg mL^{-1}, 0.5 mL) with visible light (λ_{ex} = 400–500 nm, 0.18 W, 0.21 W cm^{-2}) for 2.5 min (black trace) and 10 min (red trace). Absorbance sampled at 300 nm; peak at 24 min is the toluene internal standard.

the photochemistry of polymer **1** in $CDCl_3$ by ^1H NMR spectroscopy. Peaks corresponding to the photocleaved nitro-alkene product were observed upon irradiation by comparing the spectrum of irradiated polymer **1** to that of **3a** (Fig. S1†). However, since the photocleaved nitro-alkene product was quickly consumed by secondary photoreactions and the product precipitated (likely because of high polarity), line broadening and decreased peak heights thwarted detailed analysis.

Attenuation of visible light by dermal tissue does not prevent polymer photocleavage

To test the practical utility of one-photon visible light driven photochemistry for *in vivo* applications, we examined the efficiency of photochemistry after passage of light through hairless mouse skin (thickness: ~0.45 mm) sandwiched between two glass slides (Fig. 4a, S4†). Polymer **1** solutions were irradiated with and without this tissue filter in the beam path and the photoreaction kinetics were measured by UV-Vis absorption spectroscopy (Fig. 4b). Under direct blue light excitation (λ_{ex} = 400–500 nm, 0.18 W), the photoreaction reached 100% completion after only 10 min (Fig. 4b, open circles), whereas under skin-attenuated irradiation, the photoreaction reached 22% completion within the same irradiation time (Fig. 4b, solid circles). As the optical power reaching the sample after passage through the glass/skin tissue filter was attenuated by 82% (glass/skin = 0.03 W, skin alone = 0.06 W, Table S1†), this reduction indicates a linear correlation between optical power and reactivity of one-photon absorption, since the rate constant and reaction completion were reduced by 79% and 78%, respectively. These results thus highlight the utility of delivery systems that respond efficiently to one-photon visible light.

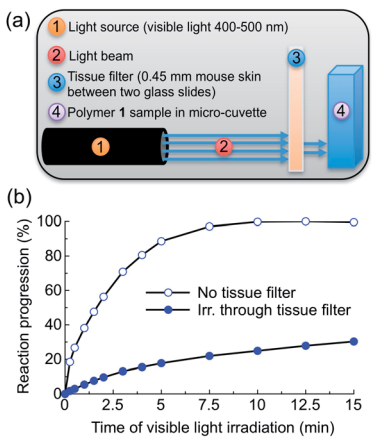

Fig. 4 Visible light triggers polymer **1** photochemistry after passage through mouse skin. (a) Experimental setup. (b) Reaction progression of CH_2Cl_2 solutions of polymer **1** (0.04 mg mL^{-1}, 0.5 mL) as they are irradiated directly (open circles) or through mouse skin (solid circles) with visible light (λ_{ex} = 400–500 nm, 0.18 W, 0.21 W cm^{-2}). The photoreactions were monitored by UV-Vis spectroscopy; the skin-attenuated reaction was further irradiated directly to fully react the polymer. Reaction progression (RP) was calculated by the following formula: $RP = ((A - A_{min})/(A_{max} - A_{min})) \times 100\%$, where A is the absorption at 490 nm, A_{min} the absorbance at 0 min, and A_{max} the maximum absorbance after complete photoreaction.

Formulation of Nile red-loaded polymeric particles and photo-induced release

As our ultimate goal is light-triggered drug delivery, we next examined release of cargo *in vitro* using Nile red as a model drug. As the traditional method of using Nile red to follow release by measuring fluorescence quenching cannot distinguish between an increase in particle hydrophilicity and cargo release, we employed a distinct approach. So that release of dye would correspond with an increase in fluorescence, we sought to encapsulate a high concentration of dye to quench its fluorescence inside the particle. For this purpose, polymer **1** was formulated into particles by electrospray[11] (see ESI† for Experimental details). This convenient formulation method produces dense, solid polymer particles in a one-step process with unrivalled payload encapsulation efficiencies, a highly desirable feature for therapeutic applications. Representative scanning electron microscopic (SEM) images of the particles are shown in Fig. S5.† We studied the kinetics of light-induced release of Nile red from polymer **1** particles (P-**1**-NR, size: 1.1 ± 0.3 μm (SEM), dye loading: 5.6% w/w) by directly monitoring changes in fluorescence intensity of the aqueous particle suspensions containing 1% w/v Pluronic® F127 upon irradiation with visible light. When P-**1**-NR was irradiated with blue visible light, a substantial increase in fluorescence intensity, indicative of photo-triggered release, was observed (Fig. 5a, solid circles). In contrast, the fluorescence intensity did not change significantly for particles not exposed to visible light (Fig. 5a, open circles). We further quantitatively measured Nile red released from particles into solution by measuring the fluorescence of the supernatant following centrifugation. We found that while only 2.0 ± 0.7% Nile red was released from non-irradiated controls, samples irradiated for 90 min released 57 ± 5% of the encapsulated Nile red, which corresponds to 1.3 ± 0.1 μg (Fig. 5b). Light-triggered release from the P-**1**-NR particles can also be followed with the naked eye, as the supernatant of centrifuged irradiated samples becomes pink, whereas non-irradiated controls display colourless supernatant as the dye is well retained in the particles without light stimulation (Fig. 5c). We also investigated whether release of Nile red continues after shorter irradiation times, but we did not observe continued release under these conditions.

The kinetics of P-**1**-NR particles' photolysis were measured by UV-Vis spectroscopy. We observed photochemical changes in P-**1**-NR particles over 60 min of irradiation, which matches well with the Nile red release kinetics (Fig. 5a, S6a and b†). When further comparing the absorption and rate of photolysis between polymer **1**, P-**1**-NR and empty polymer **1** particles (P-**1**), significant differences were observed. First, the absorbance of P-**1**-NR (λ_{max} = 475 nm) and P-**1** (λ_{max} = 438 nm) was red-shifted compared to polymer **1** in CH_2Cl_2 (λ_{max} = 398 nm). Second, photolysis rates differed considerably, that is, photolysis was complete at 10, 15 and 60 min, for polymer **1**, P-**1** and P-**1**-NR respectively (Fig. 4b, S6†). Although the particles absorb more

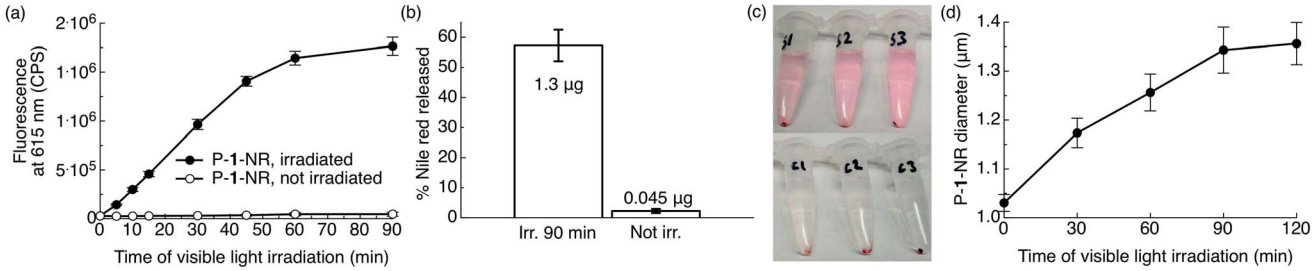

Fig. 5 Photo-triggered release of Nile red from photoexpansile polymer **1** particles (P-**1**-NR). P-**1**-NR (0.08 mg mL^{-1}, 0.5 mL, total amount Nile red per sample: 2.25 μg) in PBS (1×, pH = 7.4) containing 1% w/v Pluronic® F127 were irradiated in ambient temperature with visible light (λ_{ex} = 400–500 nm, 0.18 W, 0.21 W cm^{-2}) or kept in the dark for the same time. (a) Changes in fluorescence intensity at 615 nm (n = 3). (b) Relative and actual amount of Nile red released from the same samples after 90 min of visible light irradiation (see ESI† for calculation). (c) Photographs illustrating Nile red (pink) release from the samples/controls in (a and b) after 90 min of irradiation and after centrifugation (S1–3 = irradiated samples, C1–3 = non-irradiated controls kept in the dark). (d) Changes in particle diameter upon irradiation with visible light (Multisizer; n = 3).

visible light than polymer **1** in CH_2Cl_2, it appears that particle formulation decreases the photochemical efficiency of polymer **1**. This decrease may result from water quenching and/or close proximity of the photocages in the particle, leading to self-quenching. Furthermore, it appears that Nile red reduces the rate of photolysis, either due to inner filter effects or energy transfer from the photocages to Nile red molecules.

To examine the physical changes underlying release, the morphology, size, and structure of the particles before and after irradiation were studied by particle size analyser (Multisizer™) and SEM. Upon prolonged irradiation, we observed a progressive increase in particle diameter from 1.03 ± 0.02 to 1.35 ± 0.04 μm after 90 min of irradiation (Fig. 5d). This expansion likely results from hydrophobic-to-hydrophilic photoswitching within the particles, which leads to influx of water. Interestingly, we did not observe evidence of particle degradation or disruption by SEM (Fig. S5†), which may indicate ionic and hydrogen bonding between the photodegraded segments and/or insufficient water solubility of the photoproducts. Based on these observations, release appears to occur through increased hydrophilicity and fluidity of the particles upon amine-assisted photocleavage and photorearrangement of the polymer.

In vivo photorelease of dexamethasone from implanted depot

On-demand one-photon visible light-triggered release of biologically active agents from an implanted depot would allow local self-administration while minimizing invasive injections and systemic side effects. Furthermore, a particle depot alters the pharmacokinetic behaviour of the encapsulated cargo, allowing it to remain localized at the injection site for much longer than small molecules. Upon irradiation the cargo is released locally and on demand.

To assess the viability of the technology in animals, we examined the effect of subcutaneous light-triggered release of dexamethasone (Dex), a well-characterized anti-inflammatory drug,[12] on carrageenan-induced hind paw inflammation, a favoured model to assess the anti-inflammatory properties of potential therapeutic agents.[13]

Carrageenan, a linear sulfated polysaccharide that triggers the release of inflammatory and proinflammatory mediators, was injected into the left hind footpad of the mouse; the right hind footpad was injected with Dulbecco's phosphate buffered saline (DPBS, 25 μL) as an internal control. Using electrospray, we encapsulated Dex in photoresponsive polymer **1** particles (P-**1**-Dex, Dex loading: 1% w/w, size by SEM: 0.42 ± 0.07 μm, hydrodynamic size by dynamic light scattering (DLS): 0.95 ± 0.5 μm, Fig. S7†) along with the NIR fluorescent probe IR780 (0.1% w/w) to allow *in vivo* monitoring of the depot distribution in real time (Fig. 6a and b, S8†).

One hour prior to induction of inflammation by carrageenan, P-**1**-Dex depots were injected subcutaneously in the left hind hock. Depots were then irradiated at the injection site with blue light for 40 minutes between hind paw thickness measurements (Fig. 6c, S9†). IR780 labelling allowed tracking of the depot location by an *in vivo* imaging system (IVIS) before and after irradiation of the particles (Fig. 6b, S8†). Controls included non-irradiated P-**1**-Dex depot, DPBS with and without light exposure, free Dex, empty particles (P-**1**) and pre-irradiated P-**1** particles (Fig. S10†). The thickness of hind paws of mice injected with DPBS (Fig. 6d, S10†) increased from 0.28 ± 0.1 mm (t = 0.1 h after carrageenan injection) to a maximum of 0.71 ± 0.1 mm thicker than untreated paws (t = 5 h), while swelling in those treated with free Dex (Fig. 6d) was slightly but insignificantly (p = 0.5) lower, with a maximal difference in thickness of 0.63 ± 0.2 mm greater than control paws (t = 5 h). In contrast, irradiation of the P-**1**-Dex particle depot (Fig. 6d), led to considerably and significantly (p = 0.02) less swelling at maximal inflammation, *i.e.*, 0.44 ± 0.1 mm (t = 5 h). We hypothesize that the lower therapeutic efficacy associated with free Dex compared to P-**1**-Dex + light results from the rapid diffusion of free Dex into the systemic circulation. In comparison, the sustained light-triggered release of Dex from the implanted P-**1**-Dex depot makes it more available over time because the depot remains stationary during the experiment, as monitored by IVIS (Fig. S8†).

As we did not observe any statistically significant reduction in inflammation associated with the non-irradiated P-**1**-Dex group (t = 5 h, paw thickness = 0.72 ± 0.08 mm, p = 0.9) (Fig. 6d), we can assume that Dex stays well retained within the drug carrier. Treatment with light alone, empty P-**1** particles, or

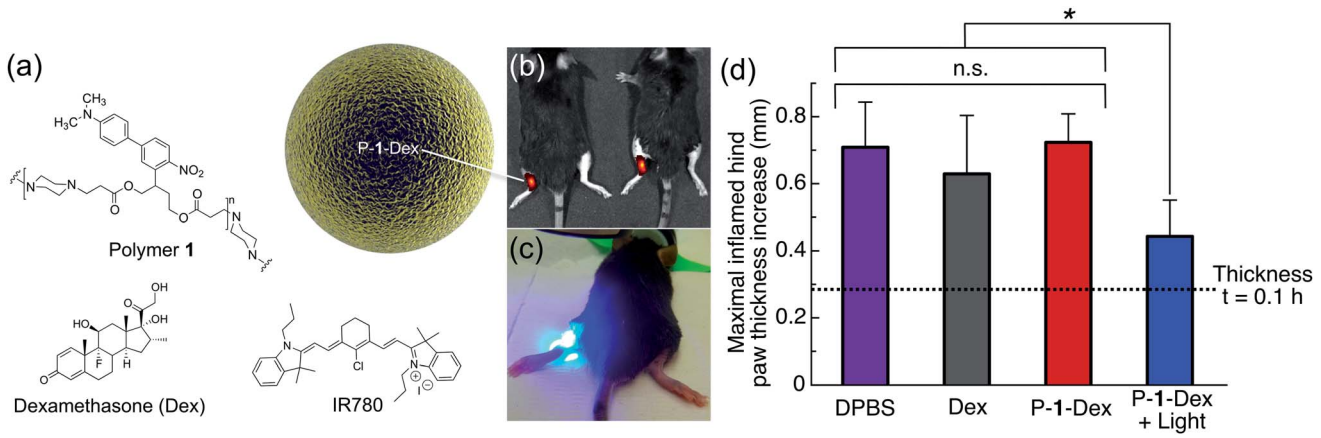

Fig. 6 One-photon visible light photo-release of dexamethasone from an implanted depot reduces carrageenan-induced hind paw inflammation in mice. (a) Composition of P-**1**-Dex particle depot. (b) Representative IVIS image of mice implanted with NIR fluorescent P-**1**-Dex depot before irradiation. (c) Photograph illustrating irradiation of the P-**1**-Dex depot with blue visible light (λ_{ex} = 400–500 nm, 0.18 W, 0.21 W cm^{-2}, 432 J h^{-1}). (d) Maximal inflamed hind paw thickness increase at t = 5 h after carrageenan injection. The P-**1**-Dex dose was 200 μg containing 2 μg Dex; free Dex dose was 2 μg; all mice were injected with a total of 25 μL of solution. n = 3 for all groups except DPBS, for which n = 6. Drug depots were injected in the left hind hock 1 h before inflammation was induced with carrageenan (2% w/v in 25 μL DPBS) in the left hind footpad. Hind paw thickness was measured using a caliper (see Fig. S9†) and the results are plotted relative to the non-inflamed right hind paw (injected at the same time with DPBS). Error bars are standard error of mean; *p = 0.02, n.s. = not statistically significant.

pre-irradiated P-**1** particles resulted in similar paw inflammation as in mice given DPBS (Fig. S10†), ruling out therapeutic effects by either light or the carrier material.

We observed no gross changes to the color or texture of the skin following irradiation (Fig. S11†). However, we observed a slight swelling (oedema) of the thigh in a few cases (Fig. S12†) that appeared to result from prolonged irradiation, which resorbed the day after light exposure. Furthermore, no signs of adverse effects from the carrier material in non-irradiated mice were apparent (Fig. S11†), in agreement with the cytotoxicity data (MTT assay) obtained for empty P-**1** particles, which showed excellent tolerance by Raw 264.7 mouse macrophage cells at concentrations up to 400 μg mL^{-1} (400 μg mL^{-1} = 115 ± 7% viability) (Fig. S13a†). However, irradiated P-**1** particles were less tolerated above concentrations of 100 μg mL^{-1} (400 μg mL^{-1} = 65 ± 30% viability) (Fig. S13a†). The free polymer **1** before and after irradiation was not as well tolerated as particles, which demonstrates that particle formulation mitigates polymer toxicity (Fig. S13b†). In conclusion, we demonstrated on-demand one-photon visible light-triggered release of an anti-inflammatory agent *in vivo*, which reduced local hind paw inflammation more efficiently than free Dex (Fig. 6d). Greater therapeutic effects might be possible with more hydrophobic drugs, which would allow higher loading efficiency.

Conclusions

This report introduces a polymer that degrades upon one-photon absorption of blue visible light, which we show enables *in vivo* photorelease of dexamethasone from a subcutaneously implanted depot of polymeric particles. Due to the altered pharmacokinetics of the implanted depot, compared to the free drug, the photoreleased Dex lowered inflammation with greater efficiency than the free drug, which rapidly diffused from the site of injection. The release mechanism appears to involve expansion of the polymeric matrix by photoinduced photodegradation and hydrophilicity switching, as demonstrated by size measurements.

The *in vivo* model used in this work demonstrates the practical utility of one-photon visible light for on-demand subcutaneous release of biological effectors. Visible light-responsive polymers and materials could become an important tool to enable light-mediated release in a multitude of animal research models.

Materials that respond to long-wavelength one-photon visible light, which is more suited for deeper tissue *in vivo* photorelease applications because of lower absorption of these wavelengths relative to the blue light used here, are currently under development.

Acknowledgements

The authors gratefully acknowledge the NIH New Innovator Award (DP 2OD006499) and King Abdulaziz City for Science and Technology (through the KACST-UCSD Center for Excellence in Nanomedicine and Engineering) for funding. NMR spectra were acquired at UCSD Skaggs School of Pharmacy and Pharmaceutical Sciences NMR facility. High-resolution mass spectroscopic data was measured at the UCSD Biomolecular and Proteomics Mass Spectrometry Facility. The authors are grateful to Dr Jacques Lux, Jessica Moore, Marlene Arredondo, Jason Olejniczak, Dr Caroline de Gracia Lux, Dr Amy Moore, Dr Shivanjali Joshi-Barr and Dr Brendan Duggan for insightful and technical help.

Notes and references

1 K. Deisseroth, *Nat. Methods*, 2011, **8**, 26.

2 N. Fomina, J. Sankaranarayanan and A. Almutairi, *Adv. Drug Delivery Rev.*, 2012, **64**, 1005; J. F. Gohy and Y. Zhao, *Chem. Soc. Rev.*, 2013, **42**, 7117; G. Liu, W. Liu and C.-M. Dong, *Polym. Chem.*, 2013, **4**, 3431; G. Pasparakis, T. Manouras, P. Argitis and M. Vamvakaki, *Macromol. Rapid Commun.*, 2012, **33**, 183; Y. Zhao, *Macromolecules*, 2012, **45**, 3647; R. Tong and D. S. Kohane, *Wiley Interdiscip. Rev.: Nanomed. Nanobiotechnol.*, 2012, **4**, 638.

3 P. Klan, T. Solomek, C. G. Bochet, A. Blanc, R. Givens, M. Rubina, V. Popik, A. Kostikov and J. Wirz, *Chem. Rev.*, 2013, **113**, 119.

4 (*a*) A. P. Goodwin, J. L. Mynar, Y. Z. Ma, G. R. Fleming and J. M. J. Frechet, *J. Am. Chem. Soc.*, 2005, **127**, 9952; (*b*) N. Fomina, C. McFearin, M. Sermsakdi, O. Edigin and A. Almutairi, *J. Am. Chem. Soc.*, 2010, **132**, 9540; (*c*) Q. N. Lin, Q. Huang, C. Y. Li, C. Y. Bao, Z. Z. Liu, F. Y. Li and L. Y. Zhu, *J. Am. Chem. Soc.*, 2010, **132**, 10645; (*d*) S. Kumar, J.-F. Allard, D. Morris, Y. L. Dory, M. Lepage and Y. Zhao, *J. Mater. Chem.*, 2012, **22**, 7252; (*e*) G.-Y. Liu, C.-J. Chen, D.-D. Li, S.-S. Wang and J. Ji, *J. Mater. Chem.*, 2012, **22**, 16865; (*f*) J. Cao, S. Huang, Y. Chen, S. Li, X. Li, D. Deng, Z. Qian, L. Tang and Y. Gu, *Biomaterials*, 2013, **34**, 6272; (*g*) W. Ji, N. Li, D. Chen, X. Qi, W. Sha, Y. Jiao, Q. Xu and J. Lu, *J. Mater. Chem. B*, 2013, **1**, 5942; (*h*) Q. Lin, C. Bao, Y. Yang, Q. Liang, D. Zhang, S. Cheng and L. Zhu, *Adv. Mater.*, 2013, **25**, 1981; (*i*) J. Olejniczak, J. Sankaranarayanan, M. L. Viger and A. Almutairi, *ACS Macro Lett.*, 2013, **2**, 683; (*j*) C. de Gracia Lux, C. L. McFearin, S. Joshi-Barr, J. Sankaranarayanan, N. Fomina and A. Almutairi, *ACS Macro Lett.*, 2012, **1**, 922.

5 C.-J. Carling, F. Nourmohammadian, J.-C. Boyer and N. R. Branda, *Angew. Chem.*, 2010, **49**, 3782; B. Yan, J.-C. Boyer, N. R. Branda and Y. Zhao, *J. Am. Chem. Soc.*, 2011, **133**, 19714; B. Yan, J.-C. Boyer, D. Habault, N. R. Branda and Y. Zhao, *J. Am. Chem. Soc.*, 2012, **134**, 16558; Y. Yang, Q. Shao, R. Deng, C. Wang, X. Teng, K. Cheng, Z. Cheng, L. Huang, Z. Liu, X. Liu and B. Xing, *Angew. Chem.*, 2012, **51**, 3125; M. L. Viger, M. Grossman, N. Fomina and A. Almutairi, *Adv. Mater.*, 2013, **27**, 3733; Y. Yang, F. Liu, X. Liu and B. Xing, *Nanoscale*, 2013, **5**, 231; M. K. G. Jayakumar, N. M. Idris and Y. P. Zhang, *Proc. Natl. Acad. Sci. U. S. A.*, 2012, **109**, 8483.

6 M. L. Denton, M. S. Foltz, L. E. Estlack, D. J. Stolarski, G. D. Noojin, R. J. Thomas, D. Eikum and B. A. Rockwell, *Invest. Ophthalmol. Visual Sci.*, 2006, **47**, 3065; W. Watanabe, N. Arakawa, S. Matsunaga, T. Higashi, K. Fukui, K. Isobe and K. Itoh, *Opt. Express*, 2004, **12**, 4203.

7 N. Z. Knezevic, B. G. Trewyn and V. S. Lin, *Chem. Commun.*, 2011, **47**, 2817; E. S. Shibu, K. Ono, S. Sugino, A. Nishioka, A. Yasuda, Y. Shigeri, S.-I. Wakida, M. Sawada and V. Biju, *ACS Nano*, 2013, **11**, 9851; M. Frasconi, Z. C. Liu, J. Y. Lei, Y. L. Wu, E. Strekalova, D. Malin, M. W. Ambrogio, X. Q. Chen, Y. Y. Botros, V. L. Cryns, J. P. Sauvage and J. F. Stoddart, *J. Am. Chem. Soc.*, 2013, **135**, 11603.

8 L. Donato, A. Mourot, C. M. Davenport, C. Herbivo, D. Warther, J. Leonard, F. Bolze, J. F. Nicoud, R. H. Kramer, M. Goeldner and A. Specht, *Angew. Chem.*, 2012, **51**, 1840.

9 S. Sun, E. A. Chamsaz and A. Joy, *ACS Macro Lett.*, 2012, **1**, 1184; C. Lv, Z. Wang, P. Wang and X. Tang, *Int. J. Mol. Sci.*, 2012, **13**, 16387; C. Lv, Z. Wang, P. Wang and X. Tang, *Langmuir*, 2012, **28**, 9387; D. Han, X. Tong and Y. Zhao, *Langmuir*, 2012, **28**, 2327; M. A. Azagarsamy, D. L. Alge, S. J. Radhakrishnan, M. W. Tibbitt and K. S. Anseth, *Biomacromolecules*, 2012, **13**, 2219.

10 S. Walbert, W. Pfleiderer and U. E. Steiner, *Helv. Chim. Acta*, 2001, **84**, 1601; D. Woll, J. Smirnova, M. Galetskaya, T. Prykota, J. Buhler, K. P. Stengele, W. Pfleiderer and U. E. Steiner, *Chem.–Eur. J.*, 2008, **14**, 6490.

11 Y. X. Xu and M. A. Hanna, *Int. J. Pharm.*, 2006, **320**, 30; A. Jaworek, *Powder Technol.*, 2007, **176**, 18; S. Chakraborty, I. C. Liao, A. Adler and K. W. Leong, *Adv. Drug Delivery Rev.*, 2009, **61**, 1043.

12 S. Tsurufuji, K. Sugio and F. Takemasa, *Nature*, 1979, **280**, 408.

13 C. J. Morris, *Methods Mol. Biol.*, 2003, **225**, 115.